ENPH 479 Assignment #1: Extreme Nonlinear Optics - Dynamics of Coupled ODEs

Matt Wright[1,*]

[1] *Department of Physics, Engineering Physics and Astronomy, Queen's University, Kingston, ON K7L 3N6, Canada*

(Dated: January 28, 2022)

The celebrated optical Bloch equations describe the dynamics of a two level quantum system interacting with an electromagnetic driving field. It is common to model such a system using the rotating wave approximation which ignores terms of "quickly varying" terms in the interaction Hamiltonian. Using computational techniques, we simulate this system to investigate the limitations of this approximation. Specifically, we examine the effects of ultrashort, high area driver pulses in which the previously ignored oscillation terms have more a significant effect due to the time-scale and magnitude of the pulse. This leads to the breakdown of the Area Theorem and the production of high frequency spectral components in the propagating pulse not captured by the rotating wave approximation.

I. INTRODUCTION

The optical Bloch equations (OBEs) describe a two-level quantum system that is interacting with an optical resonator. Such quantum systems are the basis for technologies like quantum computing. The interaction Hamiltonian depends on the electric dipole of the quantum system (often an atom) and the electromagnetic field of the classical laser. One can apply approximations and simplifications on both the OBEs and the electromagnetic field. This study uses numerical methods to simulate the effects of some of these approximations and investigate their limitations.

Computational work in [1] pioneered the connection between Rabi flopping and the breakdown of the Area Theorem under ultrashort, high intensity driver fields. Shortly after, this carrier-wave Rabi flopping phenomenon was experimental observed in GaAs [2]. Further theoretical work in [3] examines carrier-wave Rabi flopping with higher-order harmonic generation and observe a similar breakdown of the Area Theorem for larger pulse areas.

We begin by designing a fourth-order Runge-Kutta (RK4) ordinary differential equation (ODE) solver. We verify the performance of the RK4 algorithm by solving a simplified form of the OBEs. In this simplification, one assumes an on-resonance continuous wave (CW) excitation in the rotating-wave approximation (RWA), which yeilds an analytical solution. The analytical solution, RK4 solver, and a simplistic Euler ODE solver are compared.

We then begin to remove the simplifications to enter the domain of problems where there are no analytical solutions. First, using the RWA, we consider a Gaussian pulse Rabi-field, still assuming no detuning or dephasing. Here we observe a perfect Rabi flop in which the population density of the excited state (defined as the expectation value of the excited state density operator) goes from 0 to 1 and back down to 0. We then investigate the individual effects of detuning and dephasing on the maximum population density and observe different trends of decay.

Finally, we consider the full Rabi problem in which we abandon the RWA and consider an on resonance full-wave Rabi field. Firstly, the frequencies describing the quantum state transitions are varied to different multiples of the pulse area and then a phase shift is introduced to the Rabi field. Next, the laser frequency is fixed and the pulse area is changed. Finally, the power spectrum $|E(\omega)|$ is investigated by using the thin-sample approximation and analyzing the frequency domain of the real part of the coherence. This analysis is repeated for multiple pulse areas and is used to compare the custom RK4 algorithm with the `scipy` ODE solver, `odeint`.

II. THEORY AND EQUATIONS

The dynamics of a two-level quantum system can be described by the following Hamiltonian:

$$\hat{H} = \hbar\omega_0 |e\rangle\langle e| + \hbar\Omega(t)(|e\rangle\langle g| + |g\rangle\langle e|), \tag{1}$$

where the states $|e\rangle$ and $|g\rangle$ are the ground and excited states, ω_0 is the resonant frequency of the system, and $\Omega(t)$ is the Rabi frequency which describes the interaction frequency of an external electromagnetic pulse with the quantum system (e.g., the atom). This electromagnetic field is a classical laser with frequency ω_L, which we will represent as a Gaussain pulse. The Rabi frequency depends on the alignment of the electric dipole of the system and the electric field of the pulse. The rotating-wave approximation (RWA) is a simplification of this atom-field interaction wherein rapidly oscillating, counter-rotating wave terms are ignored. Explicitly, in the interaction picture of the atom-field interaction Hamiltonian, the two frequency terms arise; the counter-rotating term with frequency $\omega_L + \omega_0$ and the co-rotating term with frequency $\Delta_{0L} = \omega_L - \omega_0$. Since for near-resonance excitation, $\Delta_{0L} << \omega_L = \omega_0$, counter-rotating wave terms have a negligible effect on large enough time scales.

In the density matrix formalism, a two-level quantum system is represented by the following density operator:

$$\rho = \begin{pmatrix} n_e & \rho_{ge} \\ \rho_{eg} & n_g \end{pmatrix}, \tag{2}$$

where n_e is the expectation value of the excited state (i.e. the population density of $|e\rangle$, $n_g = 1 - n_e$ is the population of the ground state, and $\rho_{ge} = \rho^*_{eg} \equiv u$ is the coherence.

* matt.wright@queensu.ca

The density matrix formalism is applied here to account for the interaction between the two-level system and the reservoir. Such interaction could result in polarization dephasing which is taken into account below with the factor γ_d. With and without RWA, one can derive different sets of coupled ordinary differential equations (ODEs) to fully describe the density matrix in Eq. (2) – these ODEs are the celebrated optical Bloch equations (OBEs).

In the RWA, the OBEs are given by

$$\boxed{\begin{aligned}\frac{du}{dt} &= -\gamma_d u - i\Delta_{0L} u + i\frac{\tilde{\Omega}(t)}{2}(2n_e - 1) \quad (3)\\ \frac{dn_e}{dt} &= -\tilde{\Omega}(t)\mathrm{Im}[u], \quad (4)\end{aligned}}$$

where the Rabi frequency is common given by,

$$\tilde{\Omega}(t) = \Omega_0, \quad (5)$$

for continuous-wave excitation or as a Gaussian pulse,

$$\tilde{\Omega}(t) \to \tilde{\Omega}_{\mathrm{Gauss}}(t) = \Omega_0 \exp\left(-t^2/t_p^2\right), \quad (6)$$

where t_p is the pulse width. If the RWA is abandoned and the coherence is allowed to quickly vary, the full OBEs are given by:

$$\boxed{\begin{aligned}\frac{du}{dt} &= -\gamma_d u - i\omega_0 u + i\Omega(t)(2n_e - 1) \quad (7)\\ \frac{dn_e}{dt} &= -2\Omega(t)\mathrm{Im}[u], \quad (8)\end{aligned}}$$

where the full-wave Rabi field is:

$$\Omega(t) \to \Omega_{\mathrm{Gauss}}(t) = \Omega_0 \exp\left(-t^2/t_p^2\right)\sin(\omega_L t + \phi). \quad (9)$$

During the study of OBEs and pulsed Rabi oscillations, one often uses the Area Theorem to relate the pulse area to the number of Rabi cycles. The theorem states that the pulse area in Eq. (10) will produce exactly m Rabi cycles of the populaiton for a $m2\pi$ pulse.

$$A_{pulse} = \int dt\tilde{\Omega}(t) \quad (10)$$

The OBEs states above are only analytically solvable with certain restrictive simplifications on both the form of the equations and the driving field so computational techniques will be used to investigate the breakdown of these simplifications. One technique to solve the ODEs employed uses Euler's method which is a linear approximation and has an error that scales $\mathcal{O}(h^2)$ with step size, h. This is given in Eq. (11).

$$y_{n+1} = y_n + hf(t_n, y_n) \quad (11)$$

Alternatively, one can use the Runge-Kutta 4th order (RK4) ODE solver given in equations (12) to (16) which has an error that scales $\mathcal{O}(h^4)$.

$$k_1 = f(t_n, y_n) \quad (12)$$

$$k_2 = f(t_n + \frac{h}{2}, y_n + h\frac{k_1}{2}) \quad (13)$$

$$k_3 = f(t_n + \frac{h}{2}, y_n + h\frac{k_2}{2}) \quad (14)$$

$$k_4 = f(t_n + h, y_n + hk_3) \quad (15)$$

$$y_{n+1} = y_n + \frac{h}{6}(k_1 + 2k_2 + 2_k 3 + k_4) \quad (16)$$

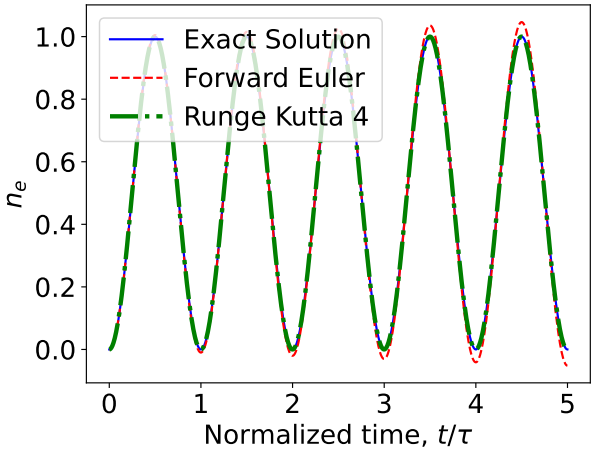

(a) $h = 0.001$

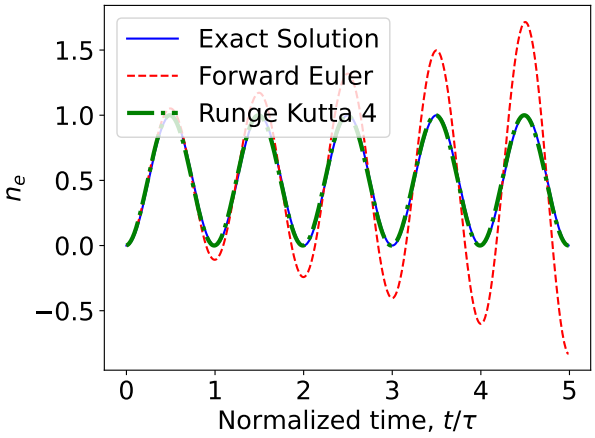

(b) $h = 0.01$

Figure 1. Comparison of analytical OBE solution with Euler and RK4 ODE solvers. Figure in (a) uses a time step size of 0.001 and (b) uses 0.01.

III. EXPERIMENTS

A. Numerical Method Verification

To introduce OBEs and verify the design of our custom RK4 ODE solver against a known analytical solution, a simple continuous wave excitation was used in the RWA. This simplification removes the time dependence of the Rabi frequency, $\tilde{\Omega}(t) = \Omega_0$. The OBEs in Eq. (3) and Eq. (4) were used with $\Delta_{0L} = 0 = \gamma_d$. The analytical solution for the excited state population in under these conditions is: $n_e(t) = \sin^2(\Omega_0 t)$ when $n_e(0) = 0$. Letting $\Omega_0 = 2\pi$, an ODE simulation was run for a total of 5 full cycles and the results of the analytical solution, a simple Euler ODE solver, and our RK4 algorithm can be seen in Fig. 1. To better observe the error of the two computational methods in Fig. 1 (a), the difference between each method and the exact solution can be seen in Fig. 2.

It is clear from these plots that the RK4 solver has superior performance, especially as the system evolves with increasing simulation time. However, it should be noted

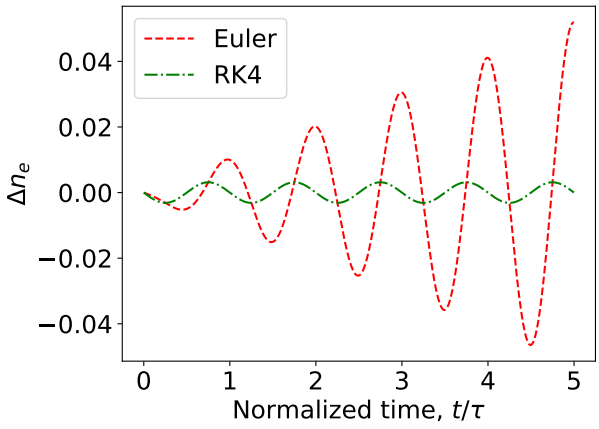

Figure 2. OBE numerical solver error over 5 cycles with step size $h = 0.001$ for the Euler and RK4 ODE solvers.

that the RK4 solver takes 4.6 times as long as the Forward Euler solver. This is an acceptable cost since RK4 simulation time for the 0.001 step size takes on the order of 0.4 s. The RK4 solver is used throughout the rest of the study.

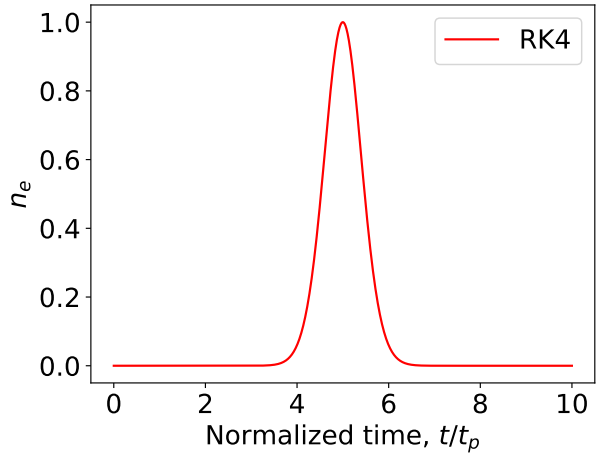

Figure 3. Excited state population for a Gaussian pulse in the RWA.

B. RWA and Gaussian Pulse

Now, still in the RWA, we consider the Rabi field represented by the Gaussian pulse defined in Eq. (6) with a pulse area of 2π. To determine the value of Ω_0 for this single Rabi flop, one can use the Area Theorem defined in Eq. (10):

$$\begin{aligned} 2\pi &= \int dt\Omega_{Gauss}(t) \\ &= \int dt\Omega_0 \exp\left(-t^2/t_p^2\right) \\ &= \Omega_0 \frac{\sqrt{\pi}}{2} \operatorname{erf}(t) \\ &\approx \sqrt{\pi}\Omega_0 \\ \therefore \Omega_0 &= 2\sqrt{\pi}. \end{aligned}$$

More generally, we have $\Omega_0 = A_{pulse}/\sqrt{\pi}$. To simulate a perfect Rabi flop we ignore dephasing ($\gamma_d = 0$) and detuning ($\Delta_{0L} = 0$) and apply a pulse with a $5t_p$ offset. As seen in Fig. 3, the excitation goes exactly from 0 to 1 and back to 0 after the pulse.

We then observe the effects of finite laser detuning and dephasing on the excitation population by individually varying both quantities. Figure 4 demonstrates decay in the maximum value of n_e for values of detuning and dephasing ranging from 0 to $\Omega_0 = 2\sqrt{\pi}$. It can be seen that dephasing decays n_e with a roughly exponentiation trend while the decay with detuning has an inflection point near the $\Delta_{0L} = \Omega_0/2$ point. Both trends are monotonically decreasing.

Figure 5 shows $n_e(t)$ over the duration of the pulse for some different values of Δ_{0L} and γ_d. Both have the effect of shifting the location of the maximum n_e values but in different horizontal directions which is likely due to the complex factor in the detuning term of Eq. (3). It can also be seen in both cases, n_e does not return exactly back to zero.

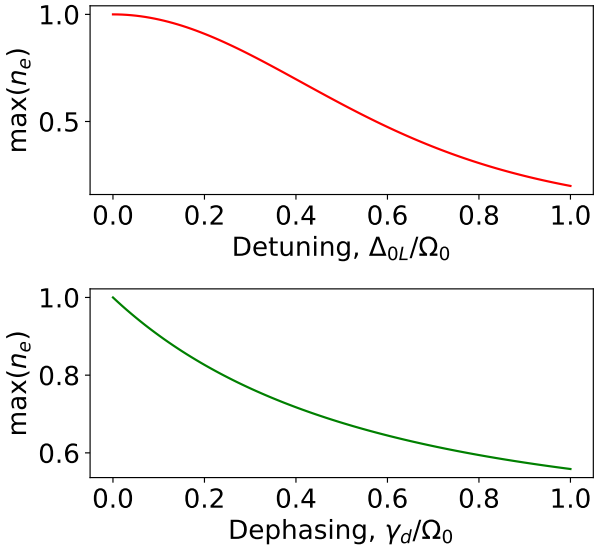

Figure 4. Comparison of the individual effects of detuning (top) and dephasing on the maximum excitation population value.

C. Full Rabi Problem

Now we consider the full Rabi problem, abandoning the RWA and allowing u to quickly vary. The dynamics of this

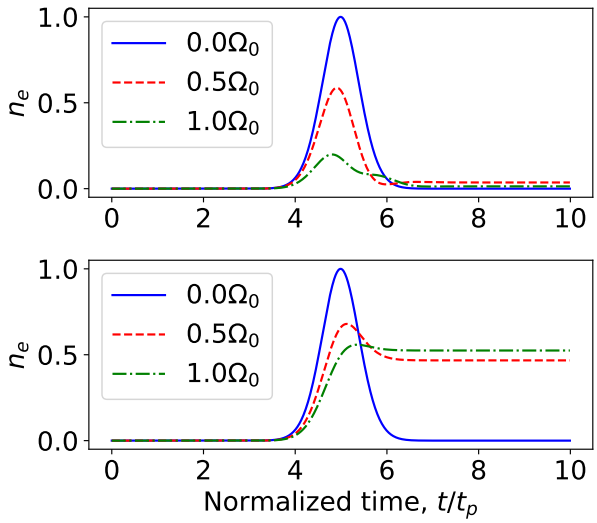

Figure 5. Comparison of the individual effects of different values of detuning (top) and dephasing (bottom) on the excitation population over the course of the pulse.

system are described in Eq.(7) and Eq.(8) with the full-wave Rabi field in Eq.(9). Staying on resonance and having $\phi = 0 = \gamma_d$, we use a 2π pulse (so $\Omega_0 = 2\sqrt{\pi}$ still) and examine the laser frequencies: $\omega_L = 20\Omega_0, 10\Omega_0, 5\Omega_0, 2\Omega_0$. Figure 6 shows the graphical results of the simulations. It is clear in Fig. 6 (a)(i.e., when $\omega_L = 20\Omega_0$) that when we have a quickly varying laser, the difference between the n_e flop with RWA (see Fig. 3) and without RWA is negligible. However, as the laser frequency decreases and begins to near the pulse area, the counter-rotating oscillations yield more appreciable effects on the time scale of the pulse. This is best exemplified by contrasting the plots in Figures 6 (a) and 6 (d) and noting that the n_e plot in 6 (a) is smooth relative to the wavy shape of that in 6 (d), signifying a departure from the results of the RWA. In Fig. 6 (d), a $\phi = \pi/2$ phase is also introduced to the $\omega_L = 2\Omega_0$ simulation. Interestingly, without the phase the maximum value of n_e was 0.986 but with the addition of the phase, a maximum n_e value of 0.999 was reached. This seems analogous to the case of a forced harmonic oscillator in which the displacement is at a maximum when the driving frequency and position frequency has a $\pi/2$ phase difference so that the driving force is in phase with the velocity. To illustrate the difference between RWA and no RWA while also compare the result of the phase shift, Fig. 7 shows the difference between the RWA n_e result and the results of the two different phase values. The difference between RWA and no RWA is certainly periodic and does not appear symmetric about the centre of the pulse. It can also be seen that phase effects the magnitude of this difference at a given time, most notably near the centre of the pulse (i.e., when $t/t_p = 5$). The RWA model cannot account for the driver phase because its derivation is rooted in the interaction picture which results in the driver phase becoming a common factor in the Rabi frequency and thus does not affect the result. It can be seen in figures 6 (d) and 7 that the drive phase essentially changes the phase of the oscillation about RWA approximation.

Now, still considering the full Rabi problem, we fix $\omega_L = 4\sqrt{\pi} = \omega_0$ and manipulate the pulse area so that Rabi frequency amplitude takes the values $\Omega_0 = 2\sqrt{\pi}, 10\sqrt{\pi}, 20\sqrt{\pi}$. The results of the experiment are shown in Fig. 8. It is clear that as the pulse area nears and exceeds the value of the driver frequency, the the system becomes more and more disturbed after the pulse. For instance, the coherence (real and imaginary components) is set into a state of oscillation from a stable value of 0 before the pulse. For n_e, the 2π pulse results in a single Rabi flop as expected (apart from some oscillation not captured by RWA), but as the pulse area increases, the breakdown of the Area Theorem can be observed. Fot a pulse area of 10π and 20π, one would expect 5 and 10 (respectively) Rabi cycles to occur but Fig. 8 (c) shows 4.5 and 9.5 cycles.

To measure the frequency content of the transmitted pulse, we employ a thin-sample approximation analyze the power spectrum of the polarization which is related to the coherence of the OBEs: $P(t) \propto \mathrm{Re}[u(t)]$. For the same 3 pulse areas discussed above (Fig. 8) we use a polarization decay rate of $\gamma_d = 0.4/t_p$, and simulate the system for $50t_p$. Then, using the `numpy` fast Fourier transform, we determine the polarization power spectrum and plot in normalized units of ω/ω_L as seen in Fig. 9. The 2π pulse has two dominant frequency components and then quickly decays while the larger area pulses show higher and lower frequency components.

IV. CONCLUSIONS

Using our analytically verified RK4 ODE solver, we have explored the limitations of the rotating wave approximation in describing the dynamics of a Rabi flopping two-level quantum system interacting with a high intensity, ultrashort electromagnetic pulse. Using a Gaussian pulse, we have simulated the optical Bloch equations with and without the rotating wave approximation. We demonstrated decrease in excitation population density resulting from dephasing and detuning in the approximation. We have shown that for high driver and resonant frequencies (ω_L and ω_0) and relatively low pulse areas, the rotating wave approximation performs well with minimal deviation from the solution of the full-wave pulse. However, as the pulse are nears and then exceeds the driver frequency, the approximation breaks down and so does the Area Theorem. Further, the rotating wave approximation does not predict the higher spectral components on the propagating wave.

References

[1] S Hughes, "Breakdown of the area theorem: Carrier-wave rabi flopping of femtosecond optical pulses," Physical review letters **81**, 3363–3366 (1998).

[2] O.D Mücke, T Tritschler, M Wegener, U Morgner, and F.X Kärtner, "Signatures of carrier-wave rabi flopping in gaas," Physical review letters **87**, 057401/4–057401 (2001).

[3] M.F Ciappina, J.A Pérez-Hernández, A.S Landsman, T Zimmermann, M Lewenstein, L Roso, and F Krausz, "Carrier-wave rabi-flopping signatures in high-order harmonic generation for alkali atoms," Physical review letters **114**, 143902–143902 (2015).

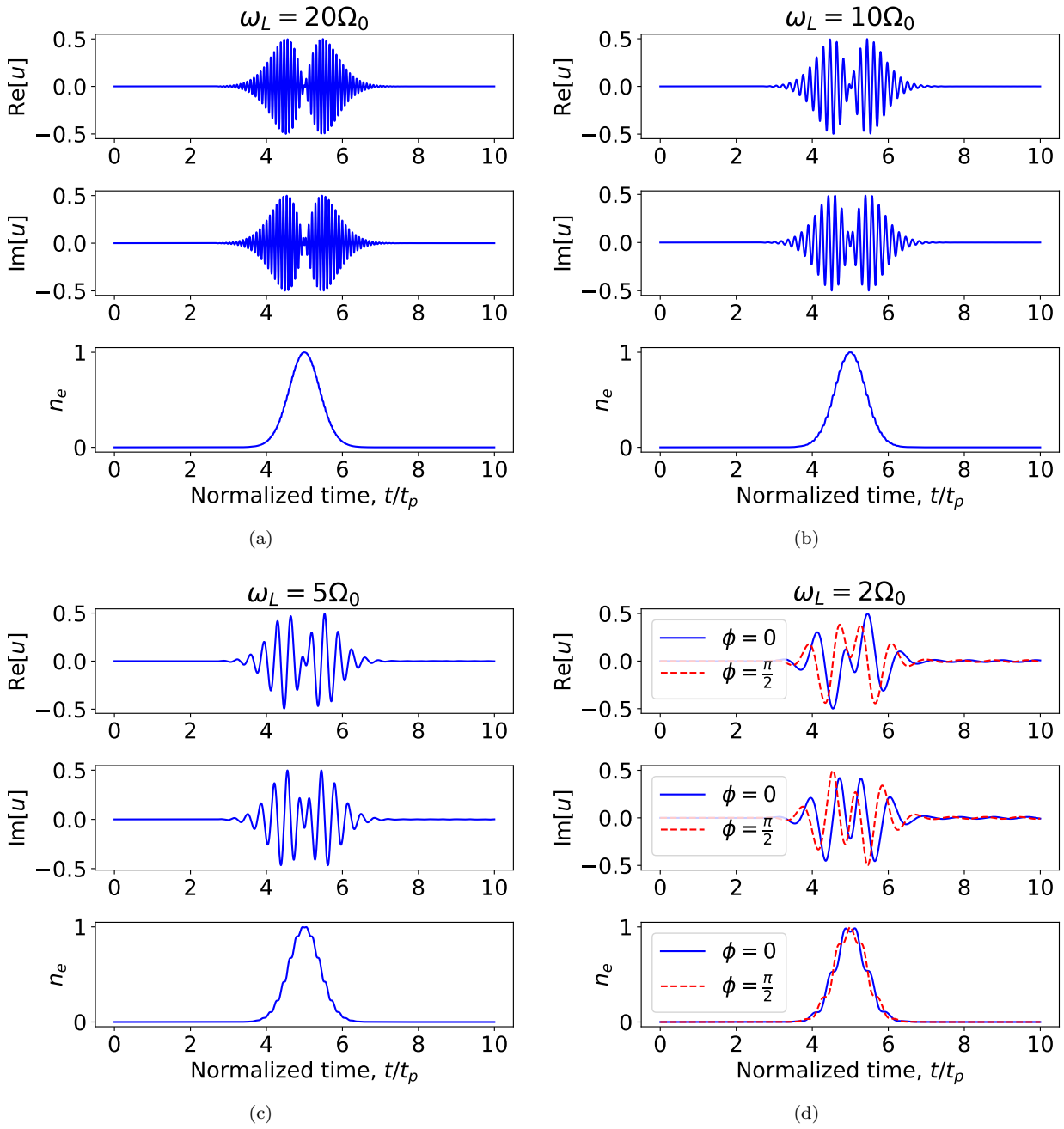

(a) (b) (c) (d)

Figure 6. Results of varying laser frequency on the excitation population and coherence.

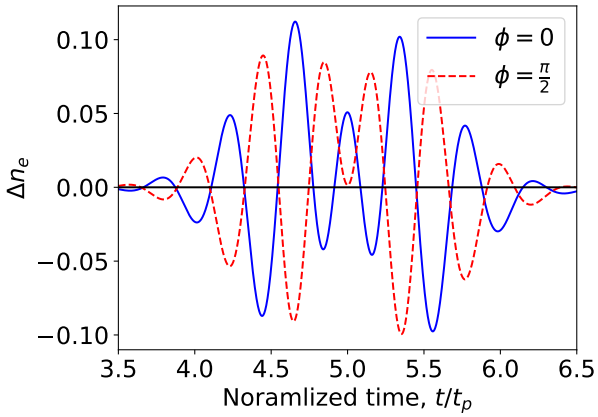

Figure 7. Difference in excitation population between RWA and full-wave Rabi field ($\Delta n_e = n_{e,RWA} - n_{e,full}$) with phase offsets of 0 and $\pi/2$.

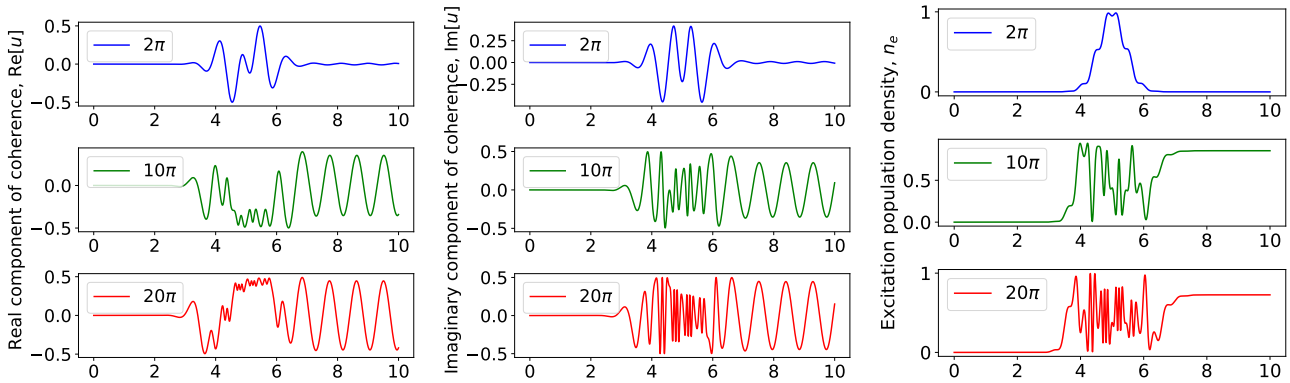

(a) Re{u} (b) Im{u} (c) n_e

Figure 8. Results of varying pulse area with $\omega_L = 4\sqrt{\pi} = \omega_0$. Pulse area takes values of 2π, 10π, and 20π.

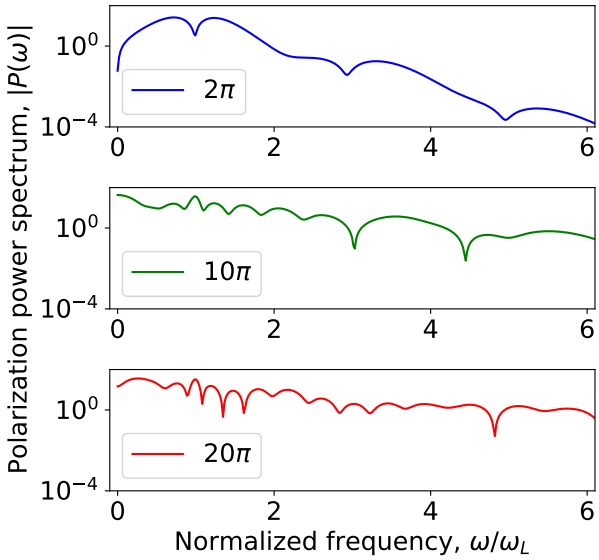

Figure 9. Power spectrum of polarization for pulse areas of 2π, 10π, and 20π with dephasing of $\gamma_d = 0.4/t_p$

.